DIRECT FOKKER-PLANCK CALCULATIONS

Haldan Cohn
Department of Astronomy
Indiana University
Swain Hall West 319
Bloomington, IN 47405
USA

ABSTRACT. The past decade has seen the development of powerful numerical methods for studying star cluster evolution by direct integration of the Fokker-Planck equation. Cohn's basic algorithm for spherical systems of identical point masses and its application to the study of core collapse is reviewed. Merritt's extension of this method to treat systems containing a mass spectrum, and Goodman's extensions to include strong scattering and rotation are discussed. Results from direct Fokker-Planck computations of core collapse in single mass and multi-mass isotropic clusters and single mass anisotropic clusters are presented to illustrate the method. Calculations of pre- and post-collapse evolution with a central black hole and with heating by hard binaries are reported. Prospects for future development of the direct Fokker-Planck method will be discussed, with emphasis on the central goal of developing physically realistic models for interpreting Hubble Space Telescope observations of globular cluster structure.

1. INTRODUCTION

During the past decade I've been involved in the development of a robust numerical method for studying star cluster evolution, based on direct integration of the Fokker-Planck equation (Cohn 1979a,b, 1980). Unlike Monte Carlo simulation techniques that produce particular stochastic realizations of the Fokker-Planck equation, the direct method reviewed here employs a finite difference scheme to obtain a time-dependent solution. The direct method is particularly well suited to investigating core collapse in star clusters and subsequent post-collapse evolutionary phases. The application of the direct Fokker-Planck method to this challenging astrophysical problem is the focus of this review.

The general redistribution of stars in phase space produced by two-body gravitational scattering was early-on recognized as the physical process that drives star cluster evolution (Jeans 1929; Ambartsumian 1938; Spitzer 1940; Chandrasekhar 1942). Following this evolution numerically presents a significant computational challenge,

J. Goodman and P. Hut (eds.), Dynamics of Star Clusters, 161–178.

since the gravitational potential in which cluster stars orbit itself evolves in time along with the evolving phase space distribution. This joint evolution was decoupled in early numerical treatments of the Fokker-Planck equation by the adoption of a square well approximation to the cluster potential. This approach allowed a calculation of the rate of escape of stars from clusters due to small angle two-body scattering (Spitzer and Harm 1958), and also permitted the development of quasi-equilibrium models for star clusters (Mitchie 1963a,b; King 1966).

Henon's (1961, 1965) path breaking similarity solutions to the self consistent evolution problem led the way to subsequent detailed numerical treatments of the Fokker-Planck equation. Larson (1970) produced the first time dependent integration of the self consistent Fokker-Planck equation using a moment equation reduction. Powerful Monte Carlo simulation methods were developed and refined in the following decade (Henon 1973, Spitzer 1975).

During the two decades following the work of Spitzer and Harm (1958), much progress was made by plasma physicists in developing direct numerical methods for solving the Fokker-Planck equation. A considerable amount of this work has been directed towards the study of particle orbit diffusion in magnetic confinement devices (Killeen, Mirin, and Rensink 1976). There is a great similarity between this orbit diffusion process and that which occurs in star clusters. Motivated by this analogy, Russell Kulsrud and I undertook the modification of a plasma kinetic Fokker-Planck code to attack the problem of determining the quasi-equilibrium stellar distribution about a massive black hole at the center of a star cluster (Cohn and Kulsrud 1978; cf. Shapiro, this volume). Buoyed by the success of this venture, Jerry Ostriker and I took on the self-consistent problem (Cohn 1979a, b). Section 2 of this review presents an overview of the direct Fokker-Planck method that resulted from this work. Extensions by Merritt (1981) to treat a mass spectrum and Goodman (1983) to include strong scattering and cluster rotation are discussed. Section 3 reviews the application of this method to the study of core collapse and cluster life thereafter. Prospects for future work are discussed in Section 4.

2. THE DIRECT FOKKER-PLANCK METHOD

The direct Fokker-Planck method is so named because it directly attacks the orbit-averaged Fokker-Planck kinetic equation for the stellar distribution function, resulting in a time-dependent solution. As discussed by Cohn and Kulsrud (1978), this kinetic equation is derived from the full Boltzmann equation under the assumption that the dynamical time is much shorter than the relaxation time. To lowest order in t_d/t_r we find that the distribution function must satisfy,

$$f = f(E, J^2, t) \tag{2.1}$$

Here E and J^2 are the specific energy and square of the specific angular momentum of a star. The time dependence of f, which is of first order in t_d/t_r, is given by,

https://doi.org/10.1017/S0074180900147369 Published online by Cambridge University Press

$$\frac{\partial f}{\partial t} = \frac{1}{P} \int \frac{dr}{v_r} \left(\frac{\partial f}{\partial t}\right)_c \qquad (2.2)$$

where $(\partial f/\partial t)_c$ is the local velocity space Fokker-Planck operator (Rosenbluth, MacDonald, and Judd 1957), v_r is the radial velocity, $P = \int dr/v_r$ is the orbital period, and the orbit-averaging integral extends between the two radial turning points of an orbit.

The Fokker-Planck equation (2.2) describes the diffusion of stars in (E,J^2)- space which is represented schematically in Figure 1.

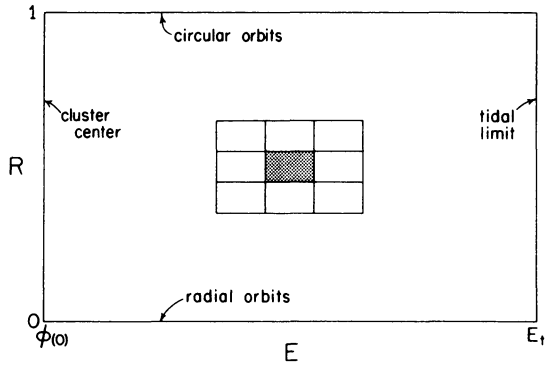

Figure 1. The domain of the orbit-averaged Fokker-Planck equation: (E,R)-space. The shaded region is a typical computational cell surrounded by eight neighbors.

It is convenient here to introduce a scaled angular momentum $R = J^2/J^2_{max}(E)$ where J_{max} is the angular momentum of a star of energy E. Each point in the rectangular region of (E,R)-space shown in Figure 1 represents a possible stellar orbit in a given spherically symmetric gravitational potential well $\phi(r)$. For the purpose of developing a finite difference form of the Fokker-Planck equation, (E,R)-space is partitioned into cells; such a cell and its eight immediate neighbors are shown in Figure 1. The occupation number for each cell is given by,

$$N(E,R) = 4\pi^2 P(E,R) f(E,R). \qquad (2.3)$$

In terms of N, the Fokker-Planck equation can be written as an equation of continuity in (E,R)-space,

$$\frac{\partial N}{\partial t} = -\nabla \cdot \mathbf{F} \qquad (2.4)$$

where $\mathbf{F}$ is the (E,R)-space particle flux vector and ∇ is the (E,R)-space divergence operator. The form of equation (2.4) indicates that only the diffusion of stars between neighboring cells (orbits) is considered in the Fokker-Planck approach.

The Fokker-Planck equation can be written in component form as,

https://doi.org/10.1017/S0074180900147369 Published online by Cambridge University Press

$$\frac{\partial f}{\partial t} = -\frac{1}{A}\frac{\partial}{\partial E}\left(D_{EE}\frac{\partial f}{\partial E} + D_{ER}\frac{\partial f}{\partial R} + D_E f\right) - \frac{1}{A}\frac{\partial}{\partial R}\left(D_{RE}\frac{\partial f}{\partial E} + D_{RR}\frac{\partial f}{\partial R} + D_R f\right) \tag{2.5}$$

where the coefficients A, D_{EE}, D_{ER}, etc. depend on E, R, and $\phi(r)$. The "D" coefficients depend additionally on f(E,R); this dependence can be written schematically as,

$$D = \int\frac{dr}{v_r}\int dE'\ G(E,E',r)\ \bar{f}(E',r) \tag{2.6}$$

where G is a particular function of the indicated arguments that can be derived from the results of Rosenbluth, MacDonald, and Judd (1957) and $\bar{f}$ is the isotropized (R-averaged) distribution function. The approximation of an isotropized background has commonly been made in stellar dynamical Fokker-Planck studies (c.f. Spitzer and Hart 1971; Marchant and Shapiro 1980), in order to simplify the computation of diffusion coefficients. However it would be possible to consider the full two-dimensional dependence of the background distribution, at the cost of some additional computational complexity, as been done in plasma kinetic studies.

Computing the evolution of a star cluster involves a self-consistent potential problem since the potential and distribution functions are related by Poisson's equation,

$$\nabla^2\phi(r) = 4\pi\ G\ \rho(r), \text{ where} \tag{2.7a}$$

$$\rho = \int d^3v\ f. \tag{2.7b}$$

Thus as f evolves in time according to equation (2.5), ϕ must also evolve. In practice, the evolution of ϕ is handled implicitly by use of adiabatic invarients. These are quantities that remain constant, to all orders of t_d/t_r, as ϕ evolves in time. Two convenient choices of adiabatic invarient are J^2 and the radial action $Q = \int dr\ v_r$. The evolution of a star cluster may be thought of as the smooth trajectory in a (f,ϕ) function space shown schematically in Figure 2. This evolution is tracked computationally by an alternating direction method indicated by the stair-step curve. The distribution function is first advanced, with ϕ held fixed, by use of a discrete form of equation (2.5). The potential ϕ is then advanced, with f held fixed as a function of adiabatic invarients, by solving equation (2.7a). This procedure is exact to second order in the time step (Cohn 1979a,b).

https://doi.org/10.1017/S0074180900147369 Published online by Cambridge University Press

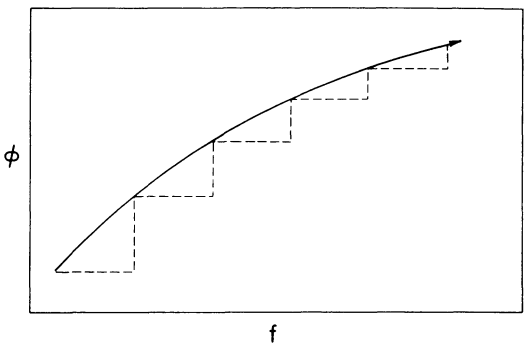

Figure 2. Schematic representation of cluster evolution in (f,ϕ)-space. The solid curve is the true trajectory while the dashed curve is the computational approximation.

The discussion to this point has focused on the two-dimensional (E,R)-space Fokker-Planck equation. As I discovered after some years in two-space, one-space is yet simpler. The two-dimensional Fokker-Planck equation (2.5) can be reduced to a one-dimensional E-space equation by averaging over R. Geometrically this amounts to projecting along the R dimension in Figure 1. Each cell in E-space now has only two neighbors. When equation (2.5) is averaged over R and zero flux boundary conditions are applied at R=0 and R=1, the energy-space Fokker-Planck equation of Henon (1961) and Cohn (1980) results. Besides significantly reduced CPU time and core storage requirements, another important advantage of the one-dimensional Fokker-Planck equation is the existence of the Chang and Cooper (1970) differencing scheme. As discussed in Section 3.3, no two-dimensional generalization of this one-dimensional scheme has been found which preserves all of its beneficial properties.

In order to treat a system with more than one mass group, an additional distribution function is added for each additional component. There is a separate Fokker-Planck kinetic equation corresponding to equation (2.5) for each distribution function, with coefficients that can be derived from the results of Rosenbluth, MacDonald and Judd (1957). Cohn (1984) and Inagaki and Wiyanto (1984) have carried out calculations of the evolution of two-component clusters, while Merritt (1981) has extended the direct Fokker-Planck method to treat systems with a continuous mass spectrum. In these three studies, the isotropized Fokker-Planck equation was used. When a large number of mass components are used, as in Merritt's (1981) study, the computation is effectively two-dimensional. Thus inclusion of the angular momentum dependence of the distribution functions would increase the dimensionality to three. This increase of computational complexity has not yet been attempted by practitioners of the direct Fokker-Planck method.

As demonstrated by Cohn and Kulsrud (1978) and by McMillan, Lightman, and Cohn (1981), the direct Fokker-Planck method can be

https://doi.org/10.1017/S0074180900147369 Published online by Cambridge University Press

extended to include additional processes besides two-body scattering by adding terms to the Fokker-Planck equation that describe loss of stars and loss or gain of energy. Such source and sink terms can often be calculated by orbit-averaging local (position dependent) rates following equation (2.2). An example of such a local rate is given by equation (3.4) below for the binary heating rate. The orbit-averaging process in this case results in an additional contribution to $\langle \Delta E \rangle$, the first order rate of charge of stellar energy.

Goodman (1983) has developed two additional extensions of the direct Fokker-Planck method: the inclusion of strong scattering in the isotropic case, and a modification of the anisotropic approach to treat axisymmetric, rotating clusters.

3. RESULTS

3.1. Core Collapse in Single Mass Systems

A particular advantage of the direct Fokker-Planck method, for studying core collapse, is the flexibility possible in zoning the orbital phase space. As discussed by Cohn (1979a,b) it is useful to adopt a uniform zoning in an auxillary function of energy which is chosen so as to allocate as many zones as desired to any interesting region of orbital phase space. As core collapse proceeds, the fractional phase space volume occupied by the cluster core becomes quite small. It is straightforward, however, to keep the number of energy zones in the core approximately constant.

The power of the direct Fokker-Planck method for studying core collapse is illustrated by Figure 3 which shows the evolution of the density profile of a single mass star cluster (Cohn 1980). This calculation used the isotropic form of the direct Fokker-Planck method discussed in Section II. The development of a power law central cusp is clearly evident in Figure 3. The slope of the cusp produced by the direct Fokker-Planck method, $d \ln \rho / d \ln r = -2.23$, is in good agreement with the value of -2.21 that was obtained by Lynden-Bell and Eggleton (1980), on the basis of the conducting gas sphere model. While the core of a globular cluster runs out of stars long before the central density has increased by 20 orders of magnitude, there will be about 10^3 stars remaining in the core when the density has increased by six orders of magnitude, assuming a total of 10^6 stars in the cluster. Figure 3 shows that the self-similar solution is well established by this time.

The long-term fate of the density cusp that develops during core collapse is a issue of fundamental importance in the study of globular cluster dynamical evolution. If a central cusp is a long-lived structural feature, then it may offer a means of identifying post-collapse clusters (Cohn and Hut 1984). Sections 3.4 and 3.5 discuss two alternative scenarios for post-collapse cluster evolution that has been investigated with the direct Fokker-Planck method: black hole driven reexpansion and three-body binary driven reexpansion.

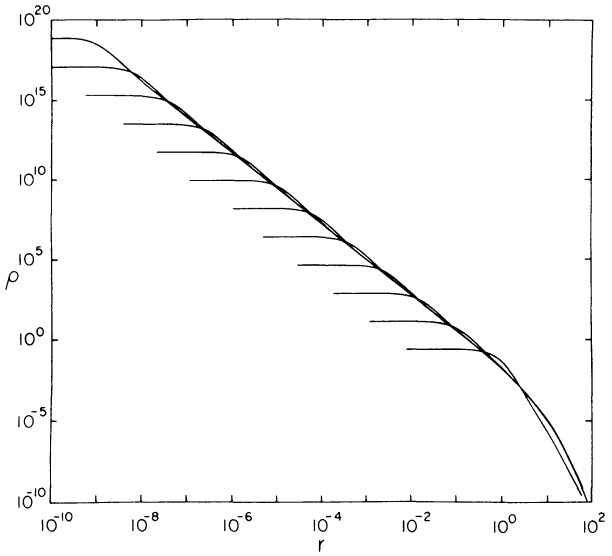

Figure 3. Evolution of the space density profile during core collapse in a single mass cluster. The central density increases in time as the core radius shrinks.

Direct Fokker-Planck calculations of core collapse have indicated an important difference between the cusp that develops as a result of core collapse and the cusp expected about a massive black hole. While the slopes of the density profiles for these two cases are similar (d ln ρ/d ln r = -2.23 and -1.75, respectively) there is a significant difference in the slopes of the velocity dispersion profiles (d ln v^2/ d ln r = -0.23 and -1.0, respectively). The much steeper cusp in velocity dispersion profile that results from the presence of a massive black hole should provide a means of distinguishing these situations observationally (cf. Bahcall and Wolf 1976).

3.2. Core Collapse in Multi-Mass Systems

Single mass models for globular clusters are clearly highly idealized, since observed mass spectra span at least a decade in mass. The isotropic direct Fokker-Planck method has been extended to treat both systems containing a small number of discrete mass components (Cohn 1984, Inagaki and Wiyanto 1984) and systems with a continuous mass spectrum (Merritt 1981). The latter study was concerned with the evolution of galaxy clusters under the action of two-body relaxation and tidal stripping and thus did not investigate core collapse in any detail. The former two studies were concerned with core collapse in a two-component star cluster and obtained similar results.

Figures 4a,b show the evolution of the space and surface density profiles for two components differing in mass by a factor of two (Cohn

https://doi.org/10.1017/S0074180900147369 Published online by Cambridge University Press

1984). The fraction of the cluster mass in the light and heavy components is 90% and 10% respectively. On the basis of Spitzer's (1969) criterion, such a cluster is expected to be unstable to mass segregation.

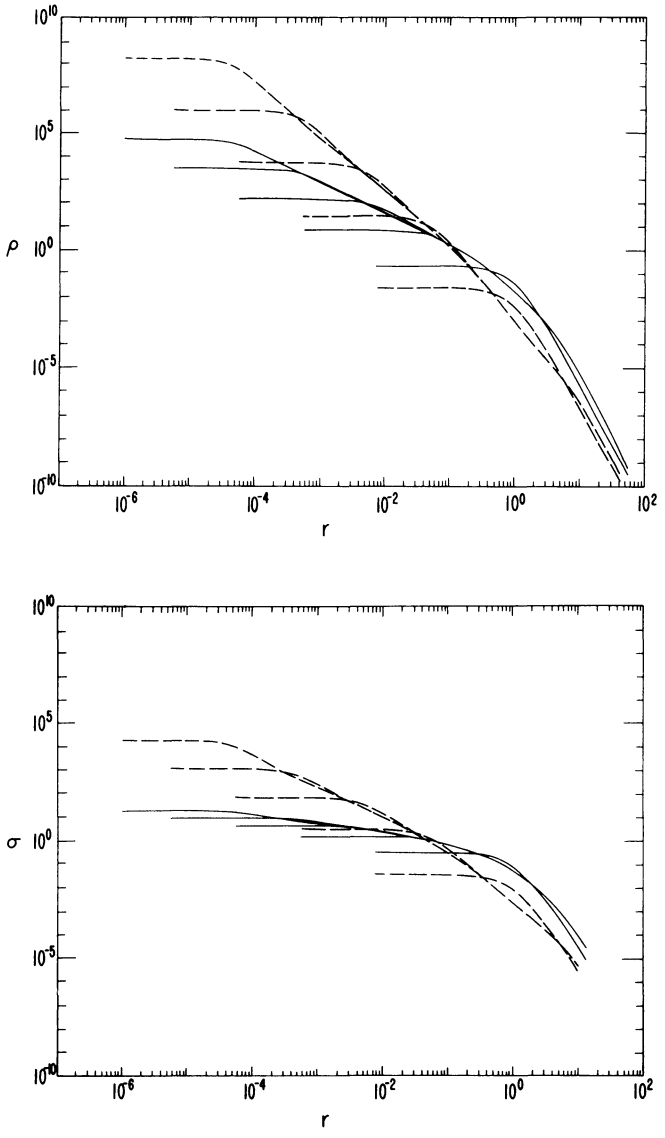

Figure 4. (a) Evolution of the space density profile during core collapse in a two-component cluster; (b) corresponding evolution of the surface density profile. Solid lines indicate the less massive component while dashed lines indicate the more massive component.

https://doi.org/10.1017/S0074180900147369 Published online by Cambridge University Press

The development of mass segregation is clearly evident in Figures 4a,b. While the two components intitially have the same density distribution (Plummer's model), the heavy component soon dominates the central part of the cluster. By the end of the computation, the evolution of the distribution of heavy stars closely resembles a one-component core collapse. In particular the slope of the heavy star cusp is d ln ρ/d ln r = -2.23, projecting to a surface density cusp slope d ln σ/d ln r = -1.23. The light stars also exhibit a central power law cusp; however the slopes of the space density and surface density are much flatter, -1.3 and -0.3 respectively. The relation between the slopes of the density cusps for the heavy and light components can be computed on the basis of the results of Bahcall and Wolf (1977) and Cohn (1980). The former study showed that if p = d ln f/d ln E, then

$$\frac{p_1}{p_2} = \frac{m_1}{m_2} \tag{3.1}$$

where the subscripts refer to mass component. Since the heavy component is distributed as in a one-component core collapse, $p_2 = 8.2$ (Cohn 1980). Denoting the density cusp slope by $\beta = -$ d ln ρ/d ln r, the gravitational potential in the central part of the cluster has slope d ln ϕ/d ln r = $2-\beta_2$, with $\beta_2 = 2.23$. Combining these results with the relation d ln ρ/d ln ϕ = p + 3/2, it follows that,

$$\beta_1 = 1.89 \frac{m_1}{m_2} + 0.35 \tag{3.2}$$

This scaling relation agrees well with the results shown in Figure 4a.

The most massive stars in a present day globular cluster are likely to be nonluminous neutron stars and heavy white dwarfs (Gunn and Griffin 1979). The stars that dominate the luminosity function -- red giants in the visual and horizontal branch stars in the UV (King 1980) -- are less massive than these nonluminous remnants. In this case, it follows from equation (3.2) that the observable surface brightness cusp that develops as a result of core collapse can be rather flatter than for a one-component cluster. Thus, depending on the mass spectrum, core collapse might occur without producing a large deviation from a normal King-type surface brightness profile.

As reviewed by Heggie elsewhere in this volume, recent conducting gas sphere model treatments of post-collapse evolution suggest that the central cusp established during core collapse evolves to a singular isothermal, $\rho \propto r^{-2}$ (Inagaki and Lynden-Bell 1983, Heggie 1984, and Goodman 1984). These studies considered a one-component cluster; if the nonluminous heavy stars in a multi-component cluster are distributed as a singular isothermal then the less massive stars will have a density gradient,

$$\beta_1 = 2 \frac{m_1}{m_2} \tag{3.3}$$

(Cohn and Hut 1984). As discussed by Djorgovski and King (1984) the

https://doi.org/10.1017/S0074180900147369 Published online by Cambridge University Press

observed surface brightness cusp in NGC 6624 is consistent with a projected singular isothermal slope of -1, although a somewhat flatter slope is also consistent with their data.

Fokker-Planck calculations of core collapse in a cluster with a continuous mass spectrum are clearly needed. Based on the results of two-component models (Cohn 1984, Inagaki and Wiyanto 1984), it seems likely that the most massive component will segregate to the center of the cluster. However if the difference in mass between components is small it is possible there may be some qualitative changes in the results.

3.3. Development of Anisotropy in Core Collapse

Comparison of the full two-dimensional Fokker-Planck calculations of core collapse presented by Cohn (1979a,b) with the isotropized one-dimensional calculations of Cohn (1980) shows few differences in the evolution up to the end of the former calculation, which corresponds to a central density enhancement by a factor of 10^3. The self-similar solution is only beginning to set in at this point. This particular set of two-dimensional calculations was terminated due to the cumulative effect of a slow but secular numerical nonconservation of energy. As discussed by Cohn (1980), adoption of the Chang and Cooper (1970) differencing scheme in the one-dimensional code reduced the energy loss rate by over two orders of magnitude. This greatly improved energy conservation permitted the isotropized calculations to be carried much farther into the self-similar regime.

Generalization of the Chang and Cooper (1970) scheme to a two-dimensional phase space has not proved straightforward. No such two-dimensional scheme appears to be available in the literature. I've investigated several alternative generalizations as has Jeremy Goodman; no scheme we've tried performs quite as well as the one-dimensional version, although all improve energy conservation relative to the simple centered differencing used by Cohn (1979a,b).

Figure 5 shows some interesting -- though preliminary -- results obtained with a two-dimensional direct Fokker Planck code using a particular heuristic generalization of the Chang and Cooper (1970) scheme. This calculation was run to an density enhancement factor of 10^6, well into the self-similar regime. The figure shows the ratio of transverse velocity dispersion to radial velocity dispersion near the onset of the gravothermal instability and at a later time. As was suggested by the earlier results of Spitzer and Shull (1975), anisotropy extends well inside the half-mass radius at late times. The degree of anisotropy at late times is not large -- about 10% -- but it is definitely present. If this calculation were to be continued beyond core collapse it is plausible that the degree of anisotropy would continue to increase. This speculation will be tested in future work.

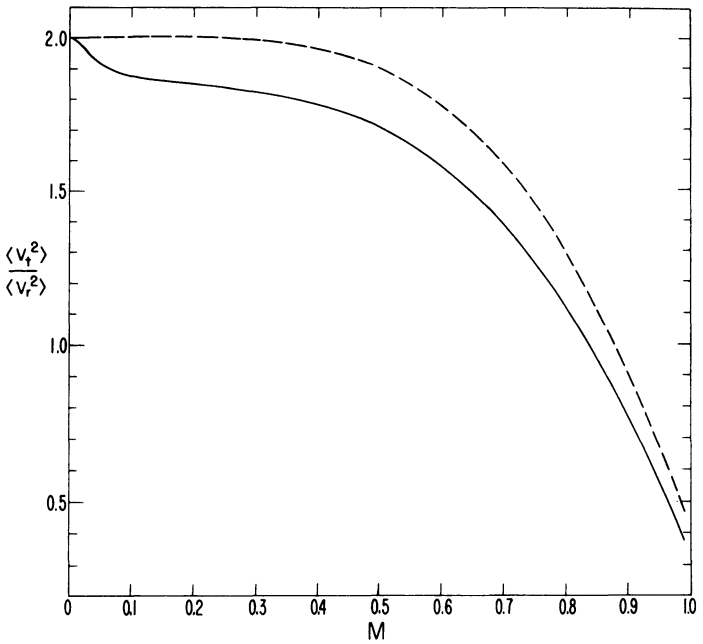

Figure 5. Evolution of anisotropy during core collapse. Abscissa is Lagrangian mass coordinate; ordinate value of 2.0 corresponds to isotropy. Dashed curve corresponds to t/t_{rh} = 12.7; solid curve to t/t_{rh} =15.8.

3.4. Post-Collapse Evolution with a Central Black Hole

As discussed by Shapiro elsewhere in this volume, the presence of a central black hole in a star cluster ultimately reverses core collapse and causes a general expansion of the cluster. It is straightforward to extend the direct Fokker-Planck method to include a central black hole by modifying the central boundary condition and adding the tidal destruction sink term given by Cohn and Kulsrud (1978). McMillan, Lightman, and Cohn (1981) have reported direct Fokker-Planck calculations of the evolution of black hole powered active galactic nuclei. Figure 6 shows previously unreported results I have obtained for the evolution of a globular cluster with a central black hole. The cluster begins as a n = 5 polytrope with a black hole mass of M_{bh} = 50 $M_\odot$ and a total cluster mass of 3 x 10^5 $M_\odot$. At the start of the run, the cusp surrounding this "seed" black hole only extends out to about 10^{-3} r_{core}. After an evolution of about 2 x 10^{10} yr, however, the combined effect of core collapse and black hole growth by accretion of tidal debris results in a cusp that extends out to about 0.1 r_{core}. (Since the profile no longer exhibits a flat core at this time, r_{core} is operationally defined as the outermost value of radius at which $d \ln \rho / d \ln r = -1.5$, which is the value at the edge of a King-type core).

https://doi.org/10.1017/S0074180900147369 Published online by Cambridge University Press

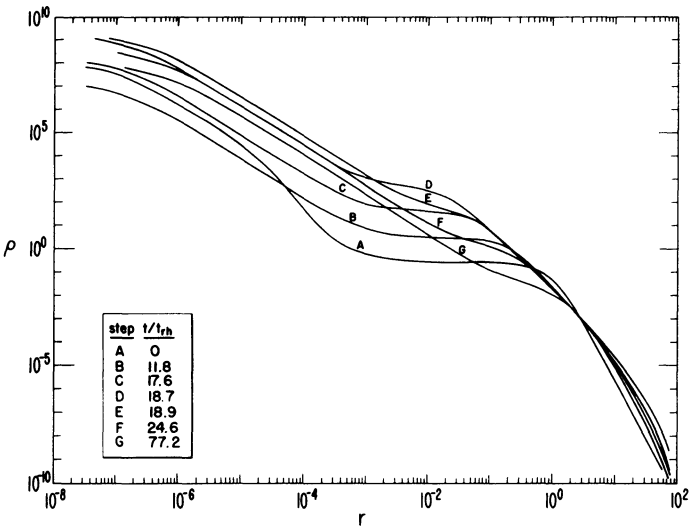

Figure 6. Evolution of density profile in a cluster containing a central black hole. For the adopted cluster structure parameters, $t_{rh} \approx 10^9$ yr.

The slope of the cusp closely agrees with the value of -1.75 first obtained by Bahcall and Wolf (1976). The collapse of the core is reversed at a time of about 2×10^{10} yr and the core radius (defined as above) gradually increases in time while the density at r_{core} decreases. Density profiles F and G in Figure 6, represent evolution times of 2.5 and 7.7×10^{10} yr respectively, indicating that the evolution rate slows markedly in the late post-collapse phase. At late times, the central black hole has grown to about 3×10^3 $M_\odot$. The density profile is characterized by a central cusp, a flatter transitional region, and an outer halo of steeper slope. This detailed structure is substantially different from that shown in Figure 3 which represents core collapse without a black hole. The cusp that develops in the presence of a central black hole also differs substantially from a normal core collapse cusp in that the velocity dispersion scales as $\langle v^2 \rangle \propto r^{-1}$ in the former case and $\langle v^2 \rangle \propto r^{-0.2}$ in the latter.

3.5. Post-Collapse Evolution with Three-Body Binaries

As Heggie has reviewed elsewhere in this volume, it now appears likely that post-collapse evolution of globular clusters is driven by energy release from hard binaries. Piet Hut and I have recently incorporated this additional physical effect into the direct Fokker-Planck method. Several alternative approaches to this extension are possible; we have investigated the addition of a heating term to the Fokker-Planck equation that is the product of the three-body binary formation rate multiplied by the total energy input per hard binary up to the time of ejection. In this approximation, hard binaries are "burned"

https://doi.org/10.1017/S0074180900147369 Published online by Cambridge University Press

instantaneously on the cluster evolution timescale. The adopted form of the heating term is

$$\dot{E} = 90\, n^2\, G^5\, m_*^5\, v_1^{-7} \qquad (3.4)$$

where $\dot{E}$ is the energy input rate per unit mass, n is the local density, m_* is the stellar mass, and v_1 is the one-dimensional velocity dispersion. Other alternatives for treating hard binaries are discussed in Section 4.

Figure 7 shows the evolution of the density profile that results with the inclusion of three-body binaries. The binary heating rate normalization was chosen for this particular run so that the total number of stars in the cluster is 5×10^4. The time corresponding to each curve in Figure 7 is given in units of t_{rh}, which is of order 10^8 - 10^9 yr for reasonable choices of core structure parameter values. For this range of half-mass relaxation times, the evolution of the system extends beyond a Hubble time.

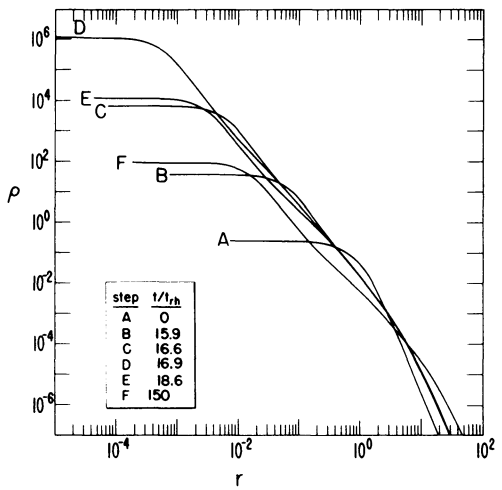

Figure 7. Evolution of density profile with inclusion of three-body binary heating.

The evolutionary sequence shown in Figure 7 begins with a core collapse phase which is halted when 27 stars remain in the core. A subsequent expansion then ensues on an ever increasing time scale; note that the time elapsed between profiles E and F is seven times longer than the time up to E.

Figure 8 shows the evolution of the density gradient profile. At the time of maximum central density (curve D) the profile is close to the $\rho \propto r^{-2.2}$ power law core collapse solution. During the subsequent expansion phase (curves E and F), no single power law characterizes the profile. Instead, d ln ρ/d ln r fluctuates between -1.9 and -2.5 for $1.5\, r_{core} \leq r \leq 300\, r_{core}$. While there is a very slight flattening

https://doi.org/10.1017/S0074180900147369 Published online by Cambridge University Press

of the profile between the initial drop off from the core and the halo it is nowhere near as pronounced as the transition region between a black hole cusp and the surrounding halo (Figure 6). The late-time cluster profiles E and F in Figures 7 and 8 resemble a $W_o = 17$ King model. While a cluster undergoing core collapse departs from the King sequence at $W_o = 8.5$ (Cohn 1980), the "ignition" of a binary heat source evidently returns the cluster to a truncated isothermal configuration of higher central concentration.

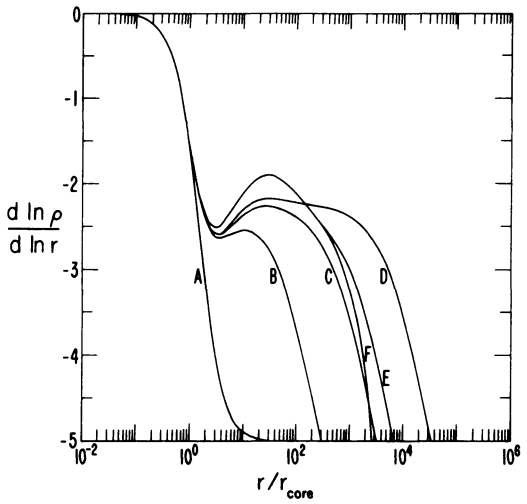

Figure 8. Evolution of density gradient profile with inclusion of three-body binary heating. The abscissa is radius scaled by instantaneous core radius. The times corresponding to each curve are the same as in Figure 7.

Figure 9 shows the time evolution of Lagrangian mass shells containing the indicated fractions of the initial cluster mass. While the core collapse process is nonhomologous, the post-collapse expansion becomes essentially homologous with the exception of the outer mass shells which are affected by the presence of an outer "absorbing" boundary. Within a few t_{rh} following core collapse, each radius expands as $\tau^{2/3}$ where τ is the time since core collapse. This scaling, which agrees nicely with predictions of Henon (1965), McMillan, Lightman, and Cohn (1981) and Goodman (1984), indicates that the time scale for energy input by binaries is equal to half mass relaxation time everywhere in the cluster. Thus, the late post-collapse phase is characterized by constant $\tau/t_{rh} = 6$ as well as constant $\tau/t_{rc} = 10^6$. During the late pre-collapse phase, only the latter ratio is constant.

https://doi.org/10.1017/S0074180900147369 Published online by Cambridge University Press

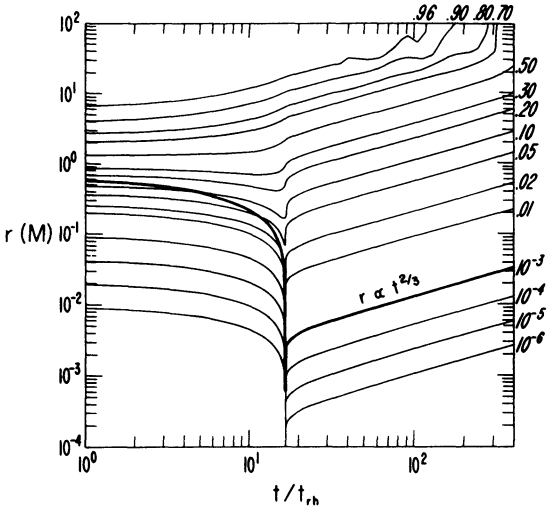

Figure 9. Evolution of mass distribution with inclusion of three-body binary heating. Light curves represent radii containing indicated mass fractions. Heavy curve represents core radius.

4. DISCUSSION

The results presented in Section 3 demonstrate the power of the direct Fokker-Planck method for investigating both pre- and post-collapse phases of globular cluster evolution. While significant progress has been made, much work remains toward the goal of constructing a evolutionary sequence of realistic cluster models. In this section I'll discuss some extensions of the work reviewed in Section 3 that are necessary for the achievement of this goal.

While two-mass direct Fokker-Planck calculations of the pre-collapse phase have been carried out (Section 3.2), no corresponding multi-mass post-collapse calculations exist. The latter calculations are crucial for predicting the surface brightness profile of a post-collapse cluster that contains nonluminous stellar remnants. A realistic mass spectrum should be adopted, with stellar mass loss that results from normal stellar evolution included (Applegate 1983). There do not appear to be any obstacles to the simultaneous treatment of these various refinements.

Most of the work reviewed in Section 3 is based on the one-dimensional (isotropized) Fokker-Planck equation. However, as described in Section 3.3, some degree of anisotropy does develop during core collapse. A two-dimensional, multi-mass calculation would provide an important test of the one-dimensional results. Such a calculation is probably best carried out using a supercomputer.

The theory of the evolution of a globular cluster with a massive central black hole now appears to be well understood. As discussed in

https://doi.org/10.1017/S0074180900147369 Published online by Cambridge University Press

Section 3.4, the cluster structure that results in this case has several unique observational signatures. Hubble Space Telescope observations of globular cluster cores should improve the observational basis for confirming or denying the presence of massive black holes in globular clusters. Should there be any positive evidence, then detailed multi-mass calculations would be in order.

The work reported in Section 3.5 on post-collapse evolution with three-body binaries represents a first step towards a full understanding of binary-driven post-collapse evolution. As discussed by Ostriker and by Stodolkiewicz elsewhere in this volume, binaries formed by two-body tidal dissipative capture should also have an important influence on globular cluster evolution. Direct Fokker-Planck calculations of the effect of this process on cluster evolution are now being carried out.

The approach for incorporating three-body binaries using a heating term discussed in Section 3.5 represents only one of several alternative treatments. A second approach that Piet Hut and I plan to implement is to use a two-species (single stars plus binaries) Fokker-Planck equation; this allows the actual distribution of binaries to be tracked in time. The detailed single-binary interaction cross sections of Hut (1983) will be used together with heuristic binary-binary cross sections. A third approach for treating three-body binaries involves tracking a small number of individual binaries using a Monte Carlo method similar to that of Henon (1975), while using the direct Fokker-Planck method for single stars. By investigating several alternative approaches for treating binaries, it will be possible to assess the robustness of the results reported in Section 3.5.

The detailed evolving globular cluster models that will result from the research program just outlined should make direct contact with observations of cluster structure. In the next few years a wealth of new data is expected to result from both ground-based and Hubble Space Telescope studies. The direct Fokker-Planck method will be a powerful tool for providing the models with which to interpret this data.

REFERENCES

Ambartsumian, V. A. 1938, Ann. Leningrad State Univ., No. 22.
Applegate, J. 1983, B.A.A.S., **15**, 920.
Bahcall, J. N. and Wolf, R. A. 1976, Ap.J., **209**, 214.
_____. 1977, Ap.J., **216**, 883.
Chandrasekhar, S. 1942, Principles of Stellar Dynamics, (Chicago: University of Chicago Press).
Chang, J. S. and Cooper, G. 1970, J. Comp. Phys., **6**, 1.
Cohn, H. 1979a, Ph.D. Thesis, Princeton University.
_____. 1979b, Ap.J., **234**, 1036.
_____. 1980, Ap.J., **242**, 765.
_____. 1984, B.A.A.S., **16**, 495.
Cohn, H. and Hut, P. 1984, Ap.J. (Letters), **277**, L45.
Cohn, H. and Kulsrud, R. M. 1978, Ap.J., **226**, 1087.
Djorgovski, S. and King, I. R. 1984, Ap.J. (Letters), **277**, L49.
Goodman, J. 1983, Ph.D. Thesis, Princeton University.
Goodman, J. 1984, Ap.J., **280**, 298.

Gunn, J. E. and Griffin, R. F. 1979, A.J., **84**, 752.
Heggie, D. C. 1984, M.N.R.A.S., **206**, 179.
Henon, M. 1961, Ann. d'Ap., **24**, 369.
_____. 1965, Ann. d'Ap., **28**, 62.
_____. 1973, in Dynamical Structure and Evolution of Stellar Systems, ed. L. Martinet and M. Mayor (Geneva: Observatory).
Hut, P. 1983, Ap.J. (Letters), **272**, L29.
Inagaki, S. and Lynden-Bell, D. 1983, M.N.R.A.S., **204**, 913.
Inagaki, S. and Wiyanto, P. 1984, submitted to Pub. Astr. Soc. Japan.
Jeans, J. H. 1929, Astronomy and Cosmogony, (Cambridge: Cambridge Univ. Press).
Killeen, J., Mirin, A. A., and Rensink, M. E. 1976, in Methods in Computational Physics, Vol. 16, ed. B. Alder, S. Fernback, and M. Rotenberg (New York: Academic Press).
King, I. R. 1966, A.J., **71**, 64.
_____. 1980 in Globular Clusters, ed. D. Hanes and B. Madore, (Cambridge: Cambridge Univ. Press).
Larson, R. 1970, M.N.R.A.S., **147**, 323.
Marchant, A. B. and Shapiro, S. L. 1980, Ap.J., **239**, 685.
McMillan, S. L. W., Lightman, A. P., and Cohn, H. 1981, Ap.J., **251**, 436.
Merritt, D. 1981, Ph.D. Thesis, Princeton University.
Mitchie, R. W. 1963a, M.N.R.A.S., **125**, 127.
_____. 1963b, M.N.R.A.S., **126**, 499.
Rosenbluth, M. N., MacDonald, W. M., and Judd, D. L. 1957, Phys. Rev., **107**, 1.
Spitzer, L. 1940, M.N.R.A.S., **100**, 396.
_____. 1969, Ap.J.(Letters), **158**, L39.
_____. 1975, in IAU Symposium 69, Dynamics of Stellar Systems, ed. A. Hayli (Dordrecht: Reidel).
Spitzer, L. and Harm, R. 1958, Ap.J., **127**, 544.
Spitzer, L. and Hart, M. H. 1971, Ap.J., **164**, 399.
Spitzer, L. and Shull, J. M. 1975, Ap.J., **200**, 339.

DISCUSSION

SPITZER: Could you please summarize the differences in behavior (density profile, rate of collapse, etc.) between your isotropic one-component model and the corresponding anisotropic model?

COHN: Apart from the modest anisotropy that develops in the latter model, there are very few differences in the results. In particular, the $\rho \propto r^{-2.23}$ law holds for anisotropic core collapse and the collapse rate is the same as for the isotropic case.

INAGAKI: How is the distribution function in the post-collapse phase? Is the Maxwellian part expanding?

COHN: I haven't yet plotted the energy dependence of the distribution function for post-collapse clusters. My impression is that there is a depletion in the distribution function at energies corresponding to the center of the potential well, so that it may be non-Maxwellian at the most bound energies.

https://doi.org/10.1017/S0074180900147369 Published online by Cambridge University Press